LA-UR- 10-0K496

Approved for public release; distribution is unlimited.

Title:	Testing and Modeling of PBX-9501 Shock Initiation
Author(s):	Kin Lam, W-13 Tim Foley, DE-6 Alan Novak, DE-6 Peter Dickson, DE-6 Gary Parker, DE-6
Intended for:	Proceedings for 14th International Detonation Symposium Coeur d'Alene, Idaho USA April 11-16, 2010

Form 836 (7/06)

Testing and Modeling of PBX-9501 Shock Initiation

Kin Lam[a], Timothy J. Foley[b], Alan M. Novak[b], Peter Dickson[b] and Gary R. Parker[b]

[a]Advanced Engineering Analysis Group, W-13
[b]Explosive Applications and Special Projects Group, DE-6
Los Alamos National Laboratory, Los Alamos, New Mexico 87545, USA

Abstract. This paper describes an ongoing effort to develop a detonation sensitivity test for PBX-9501 that is suitable for studying pristine and damaged HE. The approach involves testing and comparing the sensitivities of HE pressed to various densities and those of pre-damaged samples with similar porosities. The ultimate objectives are to understand the response of pre-damaged HE to shock impacts and to develop practical computational models for use in system analysis codes for HE safety studies. Computer simulation with the CTH shock physics code is used to aid the experimental design and analyze the test results. In the calculations, initiation and growth or failure of detonation are modeled with the empirical HVRB model. The historical LANL SSGT and LSGT were reviewed and it was determined that a new, modified gap test be developed to satisfy the current requirements. In the new test, the donor/spacer/acceptor assembly is placed in a holder that is designed to work with fixtures for pre-damaging the acceptor sample.
CTH simulations were made of the gap test with PBX-9501 samples pressed to three different densities. The calculated sensitivities were validated by test observations. The agreement between the computed and experimental critical gap thicknesses, ranging from 9 to 21 mm under various test conditions, is well within 1 mm. These results show that the numerical modeling is a valuable complement to the experimental efforts in studying and understanding shock initiation of PBX-9501.

Introduction

Explosives that are damaged by mechanical or thermal insults are thought to be more sensitive than pristine explosives because of additional porosity caused by the damage. The Nuclear Safety R&D Program at Los Alamos National Laboratory (LANL) sponsors ongoing studies aimed at understanding and quantifying this change in sensitivity by testing well characterized, pre-damaged high explosive (HE) samples and pristine samples pressed to similar bulk densities. It is expected that different damage mechanisms lead to different void morphologies (e.g., pore size distribution, cracking, channeling). Our goal is to determine how much the void morphology affects sensitivity compared to the density effect alone.

The historical LANL Small-Scale Gap Test (SSGT) and Large-Scale Gap Test (LSGT)[1] were reviewed. In these gap tests, a brass attenuator is placed between the donor explosive and the acceptor sample to be tested. The sensitivity is measured by the attenuator (gap) thickness that borders between go and no-go. The LSGT is not considered for this work because of the relatively large amount of explosives utilized. In the SSGT,

the acceptor size (0.5" diameter, 1.5" height) is desirable, but the amount of donor charge is too small to give a wide enough range of critical gap thicknesses. For example, the 50% points[1] for various samples of PBX-9501 were between 1.0 and 1.6 mm, and it would be difficult to detonate some of the less sensitive HE of interest such as the TATB based PBX-9502 in this test. We therefore increase the amount of donor explosive in the SSGT to promote larger magnitudes of the critical gap thickness and a more planar input wave into the acceptor charge. In this modified gap test, the holder is also re-designed to work with fixtures for pre-damaging the acceptor sample. Details of the test are given in the next section.

Numerical modeling is also employed in this study, to aid the test design effort as well as to develop practical and validated tools for use in system analysis codes to predict and evaluate the consequence of specific scenarios related to HE safety. The CTH shock physics code[2] developed at Sandia National Laboratories is used to calculate the wave propagation and hydrodynamic response of materials under the donor explosive loading and the possible ignition and growth of the acceptor.

In this paper, we present the modeling and test results for pristine PBX-9501 pressed to three levels of porosity. Comparison between these results and those for pre-damaged samples (to be obtained from ongoing tests) will be discussed in a separate paper.

Experimental Work

Sample Preparation

In this study, we used PBX-9501 (95 % HMX, 2.5% Estane, 2.5% BDNPA-F by weight) that was acquired from DOE stock and conformed to DOE standards. Pellets were uniaxially pressed with the pressure and duration of pressing determined by the desired density. This HE has a theoretical maximum density (TMD) of 1.86 g/cc. Samples pressed to three levels of porosity, namely 98%, 95%, and 92% of TMD, were desired. For pellets with a density of 1.83 g/cc or 98% of TMD the molding powder was heated in an oven for 15 minutes at 85°C and then pressed at 90°C at 4 ksi, 7 ksi and 10 ksi for 3, 4 and 5 minutes for each respective pressure increase, with a 1 minute time to transition between pressure steps. For pellets with a density of 1.77 g/cc or 95% of TMD the molding powder was then pressed at 24°C at 2 ksi, 6 ksi and 10 ksi for 2, 3 and 4 minutes for each respective pressure increase, again with a 1 minute time to transition from each pressure step. The lowest density examined in this experimental series was of 1.72 g/cc or 92% of TMD, which was achieved by pressing the modeling powder at 24°C at 2 ksi, 4 ksi and 6 ksi for 1, 2 and 3 minutes for each respective pressure increase, again with the aforementioned delay of one minute between steps. For each set of pellets there was a variance of ±0.002 g/cc. The pressures above were those measured on the press gauge not the pressures as applied to the surface of the pellets.

Gap Test Design

As mentioned above, the LANL historical SSGT serves as the basis of our current design. The historical design was modified so the holder for the acceptor can work with the equipment for introducing characterized thermal and mechanical damage to the sample. The donor HE was changed to PBX-9501 and made larger in diameter and height to produce a stronger and flatter driver wave into acceptor through the attenuator. Figure 1 shows the historical design while the modified design is shown in Figure 2.

In our current design, Delrin plastic was used to construct the outer assembly pieces of the experiment and Teflon was used for the inner sleeve that was in contact with the explosive under examination. The brass used to construct the gap was Muntz metal which is ~60/40 copper/zinc with a trace of iron. All gaps were 1" diameter and had a thickness that was experiment dependant. PBX-9501 at 98% TMD was used for the donor pellet, which was 0.5 inches thick and had a diameter of either 0.5" or 1". The acceptor consisted of three 0.5"-diameter 0.5"-high pellets stacked together to make an overall height of 1.5".

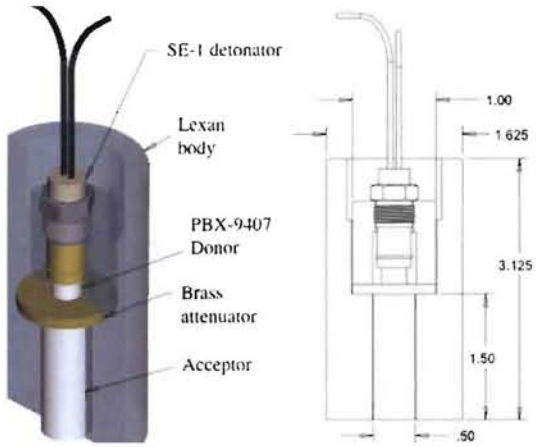

Fig. 1. LANL Historical Small-Scale Gap Test (SSGT).

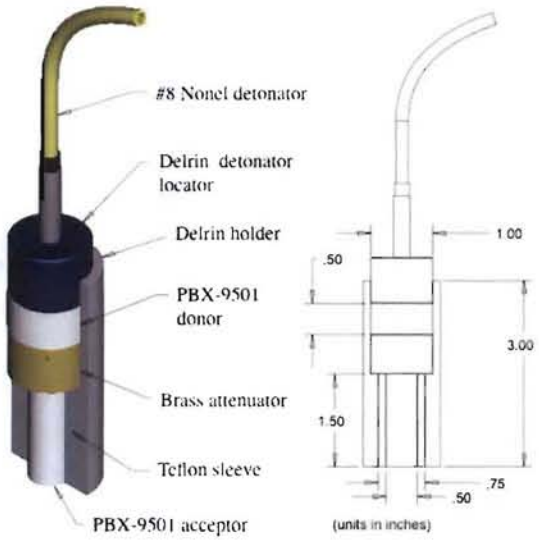

Fig. 2. Modified LANL SSGT for present work.

For the experiments where the acceptor was at 98% TMD both the 0.5" and 1" donors were used; for the experiments where the acceptor was at 95% or 92% TMD only the 1" donor was used. The donor was initiated using a non-electric blasting cap with a diameter of 8 mm. Whether a detonation occurred in the acceptor was determined by the effect on a piece of ¼ inch thick mild steel. If after the experiment there was a hole through the steel the acceptor was considered to have detonated or was a "go", if there was no hole the material was considered to have not detonated and was a "no-go". The tests were run with 1 mm increments of increasing or decreasing thickness, the selection of which was determined by the result of the previous experiment. The go/no-go point was determined by having three experiments go at one thickness and not go at the subsequent thickness. Once the mm value was established then a gap that was 0.5 mm thicker than the established go thickness was used to establish the go/no-go point to within 0.5 mm.

Experimental Results

For this experiment the distinction between a go and a no-go result was readily apparent. When a no go was observed what was presumed to be the last (bottom) pellet in the stack was recovered in either partially or totally undamaged state, so seen in Figure 3. Additionally, the steel witness plate was unmarred. When an input shock transitioned to a detonation there was a hole punched through the steel witness plate and there was no apparent explosive to recover.

Fig. 3. Image of a recovered PBX-9501 acceptor pellet in the gap test with a no-go result.

In the first experiment, where a 0.5"-diameter donor was used, the 98% TMD PBX-9501 acceptor transitioned to detonate at a gap of 9 mm, but failed to detonation at 10 mm.

In the tests with a 1"-diameter donor, the 98% TMD PBX-9501 detonated at a gap of 15 mm, but failed to do so at 16 mm. At 95% TMD, the HE sample detonated at 19 mm, but not at 19.5 mm.

At 92% TMD, the HE detonated at 20 mm, but not at 20.5 mm. In summary, we observed an increase in detonation sensitivity (i.e., thicker gaps to prevent detonation) with an increase in porosity of the HE sample, as expected. The critical gap thicknesses will be compared to modeling predictions as described in the following.

Modeling Approach

As a modeling tool we use CTH[2], which is a software package developed at Sandia National Laboratories over the past couple of decades to calculate complex phenomena involving shock wave physics. Mass, momentum and energy conservation equations for multiple materials are solved in time and space on a structured grid based on a finite-volume Eulerian method[3]. Material interfaces are tracked by high-resolution interface reconstruction algorithms based on material volume fractions. A database of equation-of-state (EOS) models is available to represent the thermodynamic behavior of a wide range of materials including explosives, metals, polymers, and gases. There are also a variety of models for material strength and fracture/failure. For high explosive detonation, programmed burn or more advanced reaction-rate based burn models can be used depending on whether the initiation time and location are known in advance.

Because of the importance of modeling HE ignition in this work, we present here the History Variable Reactive Burn (HVRB) model[4] that we adopted, which is one of several reactive burn models available in CTH (the others being Forest Fire, Ignition and Growth, Arrhenius, and the Baer-Nunziato two-phase models). Like all reactive burn models, HVRB is a composite EOS model, in which the thermodynamic state of the HE at any time is given by a linear combination of those of the initial (unreacted) and final (fully reacted, product gaseous) states, weighted by the extent of reaction, λ. The extent of reaction is in turn obtained from a history variable ϕ, defined as

$$\phi = \frac{1}{\tau_o}\int_0^t \left(\frac{P - P_I}{P_R}\right)^Z d\tau$$

$$\lambda = \min\left(1, \phi^M\right)$$

where P is pressure and t and τ represent time. HVRB is an empirical model based on the critical energy concept, and the parameters P_I, P_R, Z and M are determined from wedge test data. The parameter τ_o (not independent) has been chosen to be 1 μs to make the history variable dimensionless.

CTH Model of Gap Test

CTH modeling was incorporated early in the test development process, including simulation of the LANL historical SSGT and some candidate test designs. As the design was finalized, prediction of the critical gap sizes for the modified test was made. For each test with a specified donor size and acceptor density, the attenuator thickness was varied in the CTH model to find the critical gap size, i.e., the go/no-go boundary.

A schematic of the 2D axi-symmetric model of the modified LANL Gap Test is shown in Figure 1, which also includes selected tracer points in various materials where time histories of solution variables are recorded for post-processing. Details of the detonator are ignored; it is represented simply by a 0.3"-high, 0.3"-diameter PETN pellet. A programmed burn model with the JWL EOS model is used to initiate and propagate the detonation from the top of the pellet at time zero. HVRB for PBX-9501 is used to model the burn behavior of both the donor and acceptor, with the unreacted HE represented by a Mie-Gruneisen EOS and the product gas by a SESAME tabular EOS. We do not have an EOS model for Delrin, so a similar plastic Nylon is used to model the holder and detonator locator as a Mie-Gruneisen EOS for this material is available in the database. The Mie-Gruneisen EOS model is also used for the other solids, including the brass attenuator, Teflon sleeve, and steel witness plate. Strength is modeled only for the attenuator and witness plate, with the viscoplastic Johnson-Cook model. Table 1 gives a summary of the material models used in the gap test model.

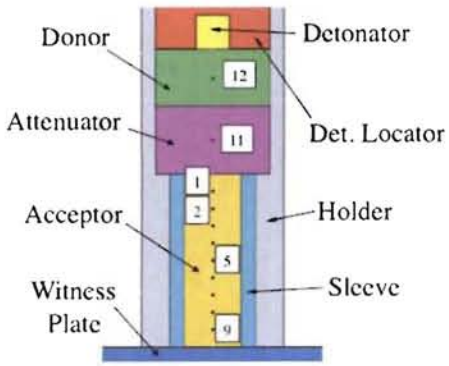

Fig. 4. Initial material distribution of axi-symmetric CTH model with locations of selected time-history tracer points. Tracers 1, 2, 5, and 9 are 3.8, 7.6, 19.1, and 34.3 mm, respectively, from the top of the acceptor; tracers 11 and 12 are in the middle of the attenuator and donor.

Table 1. EOS and strength models used in CTH simulations of the gap test.

Material	EOS	Strength
PBX-9501	Mie-Gruneisen + SESAME (HVRB)	None
PETN	Programmed Burn with JWL	None
Brass	Mie-Gruneisen	Johnson-Cook
Steel	Mie-Gruneisen	Johnson-Cook
Teflon	Mie-Gruneisen	None
Nylon	Mie-Gruneisen	None

All of the material model parameters are from the CTH database library. For the PBX-9501 HVRB model, the parameters are

$P_R = 7.60$ GPa, $P_l = 0.1$ GPa, $Z = 2.7$, $M = 1.2$

These are for PBX-9501 at the nominal density of 1.83 g/cc (98% TMD). At other densities, it was suggested based on previous studies[4] that the parameter P_R may be scaled with the density as

$$\frac{P_R}{P_{Ro}} = \left(\frac{\rho}{\rho_o}\right)^4.$$

Hence the values of P_R for PBX-9501 at 1.77 g/cc (95% TMD) and 1.72 g/cc (92% TMD) are 6.71 and 6.16 GPa, respectively. The decreased values of P_R will account for the increased sensitivity due to porosity as the density is decreased.

Modeling Results

We first discuss the simulation results for the test with a 1"-diameter donor and acceptor of PBX-9501 at 98% TMD. Figure 2 shows qualitatively how the pressure develops after ignition of the detonator. This is for the case with a attenuator thickness of 15 mm. At 0.5 μs, the detonation wave in the detonator is about halfway down its height. The detonation is ignited at the top surface of the PETN pellet and is propagated with the programmed burn model. This pressure wave initiates the donor PBX-9501, resulting in a detonation as shown in the plot at 2 μs. The driving pressure from the donor then propagates across the brass attenuator and enters the acceptor (see plots at 5 and 6 μs). As for the donor, the reactive burn of the acceptor PBX-9501 is calculated with the HVRB model. At 8 μs, we can see that the acceptor has been initiated. The detonation then propagates down the acceptor, as shown in the plot at 10 μs.

Figure 3 shows the pressure histories at three tracer locations (#1, #11, #12; see Figure 1). The characteristic detonation wave in the donor (P.12) is clearly visible, with a peak pressure of 501 kbar at 1.7 μs. The transmitted shock wave in the attenuator (P.11), with a peak of 243 kbar at 3.9 μs is also evident. In the acceptor (P.1), the pressure first jumps to 61 kbar at 6.5 μs as a result of the input wave, then increases due to beginning of the reactive burn. The reaction does not complete, however, until the arrival of additional pressure input from reaction further down the acceptor, resulting in the pressure spike of 362 kbar at 9 μs. Tracer #1 at 3.8 mm from the gap is within the run distance to detonation.

Figure 4 plots the extent of reaction for four tracers in the acceptor. We can see that reaction at tracer #2 starts later than tracer #1 but goes to completion very fast and sooner than tracer #1. From examination of a time sequence of λ contour plots, the reaction is seen to first reach completion at 7.3 μs, after a run distance of 7 mm. The detonation becomes steady about halfway down

the acceptor. From the λ curves for tracers #5 and #9 (separated by a distance of 15.2 mm), the detonation velocity is calculated to be 8.51 km/ s.

If the gap thickness is increased to 16 mm, the reaction will fail to grow. Figure 5 plots P.1 in this case together with the 15-mm case. It can be seen that the pressure rise of 55 kbar in this case is 6 kbar lower than in the 15-mm case because of the thicker attenuator. No pressure spike due to subsequent detonation is seen. The extents of reaction for the two cases are compared in Figure 6, showing the reaction failing to grow beyond about 30% completion in the 16-mm case.

Figure 7 shows the distribution of materials in the two cases at the beginning and end of the simulation at 20 μs. Denting of the witness plate due to detonation of the acceptor is clearly evident in the 15-mm case.

Simulations were made with additional gap thicknesses, in steps of 0.25 mm. It was found that the acceptor detonates at a gap thickness of 15.75 mm but fails to detonate at 16 mm (as discussed above). Mesh convergence studies with grid resolutions of 0.2, 0.1, and 0.05 mm were performed to verify that the computed critical gap thicknesses are not affected by numerical discretization or truncation errors.

Following the same procedure as above, we simulated three other tests: 1"-diameter donor with 95% and 92% TMD PBX-9501 acceptors, and 0.5"-diameter donor and PBX-9501 acceptor at 98% TMD. The calculated critical gap thickness results are summarized in Table 2, together with the experimentally observed values. Like in the experiments, the calculations show thicker critical gaps (for a fixed donor size) as the acceptor HE density decreases indicating a higher sensitivity. When the donor diameter is reduced, the critical gap becomes thinner, as expected. The agreement between simulation and experiment in all cases to less than 1 mm in the critical gap thickness is excellent.

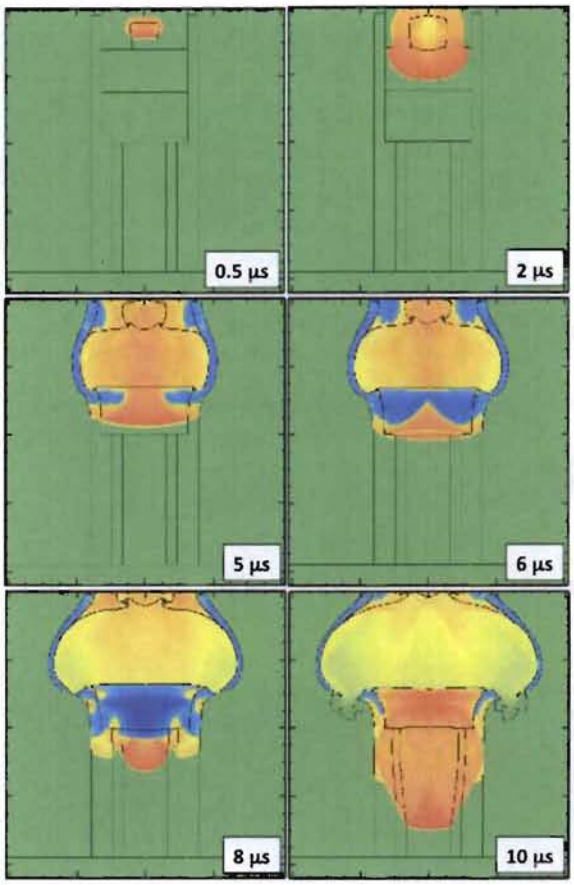

Fig. 5. Developing pressure profiles for test with 15-mm gap and 98% TMD PBX-9501. Red color represents high positive pressure (about 500 kbar maximum) and blue color represents low negative pressure (about -100 kbar minimum).

Additional quantitative results are obtained from the simulation of tests with the 1"-diameter donor and acceptor PBX-9501 samples at three densities. The results, which are shown in Table 3, include the peak pressure at tracer #9, which is 34.3 mm from the top of the acceptor (see Figure 1). In all three cases, the gap is not thick enough to prevent detonation of the acceptor. As expected, the calculations show that both the detonation pressure and velocity decrease as the density of the acceptor decreases.

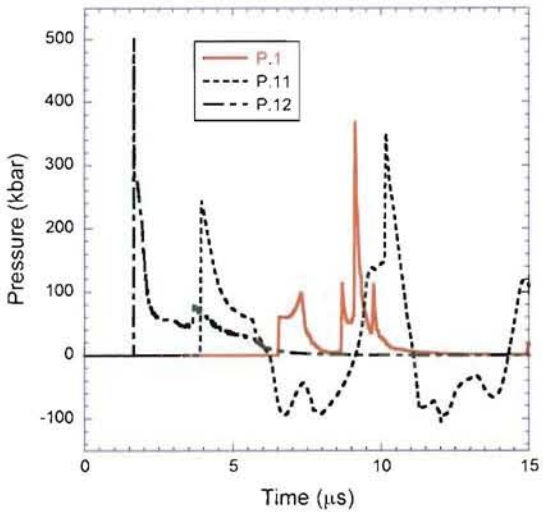

Fig. 6. Pressure histories at three tracer points (in acceptor, attenuator, and donor) for test with 15-mm gap and 98% TMD PBX-9501.

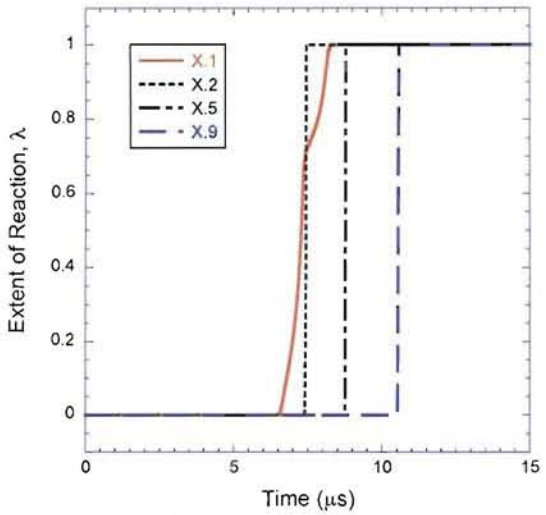

Fig. 7. Extent of reaction in acceptor for test with 15-mm gap and 98% TMD PBX-9501.

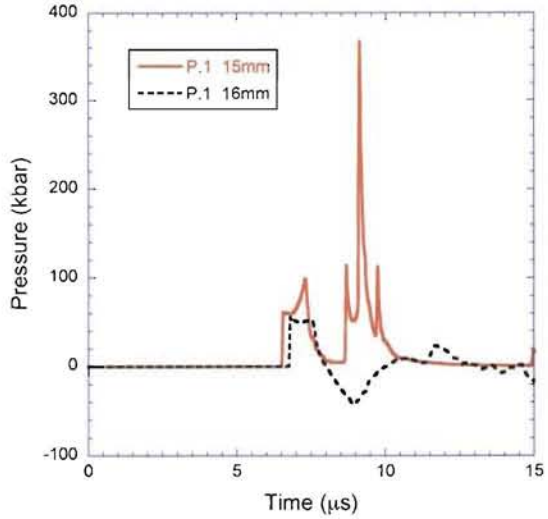

Fig. 8. Pressure history at tracer 1 in the acceptor for tests with 15-mm and 16-mm gaps and 98% TMD PBX-9501 showing no pressure spike for the thicker-gap case because of failure to detonate.

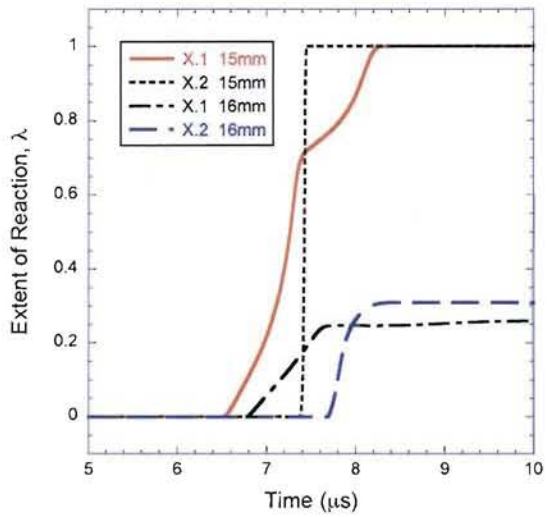

Fig. 9. Extent of reaction in acceptor for tests with 15 mm and 16 mm gaps and 98% TMD PBX-9501 showing incomplete reaction for the larger-gap case.

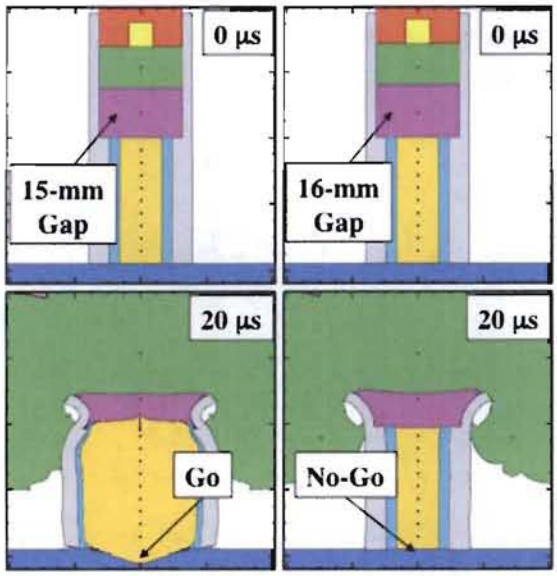

Fig.10. Material distributions at initial and final simulation times for tests with 15-mm (left) and 16-mm (right) gaps and 98% TMD PBX-9501.

Table 2. Summary of calculated and experimental critical gap thicknesses for two donor diameters and three acceptor PBX-9501 densities.

Density (g/cc)	Donor Size (in)	Critical Gap Thick. (mm)			
		CTH		Experiment	
		Go	N.G.	Go	N.G.
1.83	0.5	9.25	9.5	9	10
1.83	1.0	15.75	16	15	16
1.77	1.0	18.75	19	19	19.5
1.72	1.0	20.75	21	20	20.5

Table 3. Calculated peak pressure at tracer #9 and detonation velocity for PBX-9501 acceptor at three densities.

Density (g/cc)	Gap Size (mm)	Peak P.9 (kbar)	Detonation Velocity (km/s)
1.83	15	415	8.51
1.77	18.75	356	8.06
1.72	20.75	327	7.98

Conclusions

We have developed a modified gap test based on the LANL historical SSGT for studying HE detonation sensitivity. Quantitative results were established of the sensitivities of pristine PBX-9501 pressed to three levels of porosity (98%, 95%, and 92% TMD). The sensitivity was shown to increase with an increase in porosity. This trend was expected as more porosity promotes more hot spots for initiation. CTH calculations with the HVRB reactive burn model were performed to simulate the tests. The modeling and experimental results agree very well, to within 1 mm in the critical gap thicknesses, which range from 15 mm to 21 mm for a 1"-diameter donor.

Ongoing efforts are being made to prepare and test PBX-9501 samples that are damaged thermally to similar levels of bulk porosity as above. The results will be compared against those of the pristine samples to help understand how damage affects sensitivity. Simulation with CTH and its HVRB and additional models will be a valuable tool in this endeavor.

References

1. Urizar, M.J., Peterson, S.W. and Smith, L.C., Detonation Sensitivity Tests, Los Alamos Scientific Laboratory Report LA-7193-MS, April 1978.

2. Crawford, D.A. et al., *CTH User's Manual and Input Instructions, Version 9.0*, Sandia National Laboratories, January 2009.

3. McGlaun, J.M., Thompson, S.L., Kmetyk L.N. and Elrick, M.G., "CTH: A Three-Dimensional Shock Wave Physics Code," *Int. J. Impact Engng.*, Vol.10, pp.351-360 1990.

4. Hertel, Eugene S., and Kerley, Gerald I., *CTH Reference Manual: The Equation of State Package*, Sandia National Laboratories Report SAND98-0947, pp 57-59, April 1998.